Robotic sequential ultrasonic welding of thermoplastic composites: Process development and testing

Choudhary, A.; Villegas, I.F.

Publication date
2021

Document Version
Accepted author manuscript

Published in
Proceedings of the ASC 36TH Annual Technical VIRTUAL Conference

COVER SHEET

Title: *Robotic sequential ultrasonic welding of thermoplastic composites: Process development and testing*

Authors:

1. Abhas Choudhary M.Sc., Aerospace Structures and Materials Department, Delft University of Technology
2. Dr. Irene Fernandez Villegas, Aerospace Structures and Materials Department, Delft University of Technology

PAPER DEADLINE: ****July 1, 2021****

PAPER LENGTH: ****14 Pages****

SUBMISSION PROCEDURE: **Information on the electronic submission of manuscripts is provided on the conference web site.**

INQUIRIES TO: **See Editor**

We encourage you to read attached Guidelines prior to preparing your paper—this will ensure your paper is consistent with the format of the articles in the Electronic product.

NOTE: Please submit your paper in Microsoft Word® format or PDF if prepared in a program other than MSWord. Sample guidelines are shown with the correct margins. Follow the style from these guidelines for your page format.

Electronic file submission: When making your final PDF for submission make sure the box at "Printed Optimized PDF" is checked. Also—in Distiller—make certain all fonts are embedded in the document before making the final PDF.

Faculty of Aerospace Engineering, Delft University of Technology, Kluyverweg 1 2629HS Delft,The Netherlands

ABSTRACT

Multi-spot sequential ultrasonic welding is a promising joining technique for fibre-reinforced thermoplastic composites structures (TPC). In existing research on the multi-spot sequential ultrasonic welding process, welds are produced through the use of a static table-top welding machine, at a coupon level. However, in order to apply this joining technology to large structures, the welding process needs to be up-scaled through the use of a robotic platform.

At the Smart Advanced Manufacturing (SAM|XL) automation field lab and TU Delft Aerospace Engineering, a robotic sequential ultrasonic welding system has been developed. The system consists of a welding end-effector (EEF) equipped with various sensors that enable online process monitoring and control, which can be mounted on an industrial robot arm to perform sequential multi-spot welds. The goal of this study was to assess the welding performance of the ultrasonic welding EEF, which was mounted on an industrial KUKA KR210 R2700 Extra 10-axis robot arm, by comparing it to the performance of welds produced through the static table-top machine.

In this study, single and multi-spot welds were produced on thermoplastic composite coupons, based on welding conditions which were defined in a preliminary study. The robot and EEF deflections observed during the welding process were analysed to assess the deviation of the robotic process from the static one. The feedback obtained from the welding equipment in terms of consumed power and tool displacement in both processes was also compared. The weld quality was assessed though single lap shear testing of the welded joints as well as fractography of the failure surface. The results of this study indicate that the developed robotic welding process is quite robust and is capable of producing high-quality sequential welded joints despite significant system deflections observed during the welding process. Slightly lower welded area and weld strength was obtained which can be attributed to the system deflections. Finally, the results indicate that the use of a stiffer robotic platform as well as a stiffer EEF construction will result in better system rigidity and weld spot positioning accuracy, and through this the welding process shows promise for large-scale industrial applications.

Faculty of Aerospace Engineering, Delft University of Technology, Kluyverweg 1 2629HS Delft,The Netherlands

INTRODUCTION

Thermoplastic composites (TPC) have drawn significant interest in the aerospace and automotive industries due to their high fracture toughness, chemical and solvent resistance, infinite shelf life, recyclability and weldability. Ultrasonic welding (USW) is an attractive welding technique for TPC structures due to shorter process times and no requirement of a foreign material at the joint interface [1]. The welding process is characterized by a vibration phase and a consolidation phase. During the vibration phase, a metallic sonotrode is used to apply a static force on the intended weld area, while exerting high-frequency and low-amplitude vibrations. These vibrations heat up the interface through surface friction and viscoelastic heating [2,3]. To focus the heat generation at the weld interface, an energy director (ED) is used. Typically, the energy director is made from the same polymer as in the adherends, in the form of either a flat film, woven mesh or moulded triangular protrusions [4]. Due to the lower stiffness of the ED, it experiences higher cyclic strains than the adherends, which promotes a larger heat generation at the interface [5]. During the consolidation phase, the static force is maintained without further vibrations, to allow for solidification of the molten polymer at the interface and to avoid the generation of voids in the joint interface or the adherends.

The process can be used to consistently achieve high joint strengths in very short process times (0.1-1.5 seconds). Multi-spot welded (MSW) single-lap joints have been demonstrated to exhibit a comparable load-carrying capability as well as a more localized damage upon failure, when compared to mechanically-fastened joints of similar size, owing to higher joint stiffness and lower secondary bending and peel stresses [6,7]. It is also expected that MSW joints exhibit a higher damage tolerance over continuously welded seams due to a potential inherent crack arresting behaviour as a result of discontinuity in the joints and the need for a crack to re-initiate in subsequent welded spots. Hence, sequential multi-spot ultrasonic welding is a promising joining technology for industrial application, provided that the process can be automated for the assembly of large structural components with complex geometry. In particular, this process shows potential for application in the sub-assembly of the lower shell of a full-scale thermoplastic composite fuselage demonstrator as part of the Clean Sky 2 Joint Undertaking (JU) funded STUNNING project [8]. In the project, the lower half of the stiffened fuselage skin shall be joined to frames using structural clips which shall be sequentially welded in the demonstrator, as shown in Figure 1. The STUNNING project consortium comprises of various members, as shown in Figure 1 (left).

In this work, the performance of an end-effector developed for upscaling the ultrasonic spot welding process based on robot actuation was analysed and compared to the static table-top welding process. Single and sequential-spot welds were performed on flat thermoplastic composite specimens in single-lap shear configuration. Robot deflections and power-displacement data captured by the integrated sensors of the welding machine were analysed to understand the similarities and difference between both processes. The quality of the welded joints was tested by single-lap shear tests as well as fractography of the failure surface.

Faculty of Aerospace Engineering, Delft University of Technology, Kluyverweg 1 2629HS Delft,The Netherlands

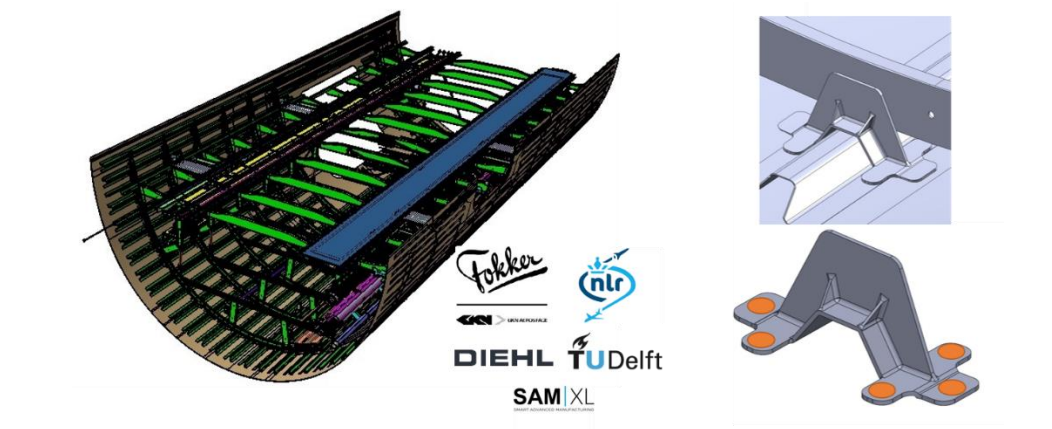

Figure 1: Lower shell of the fuselage demonstrator (left) and clip-stringer-fuselage skin joint with weld locations highlighted (right)

EXPERIMENT PROCEDURE

Materials and manufacturing

In this study, Toray Cetex® TC1225 uni-directional fibre-reinforced low-melt PAEK pre-impregnated tapes was used to manufacture the TPC adherends. The plies were stacked according to a $[0/90]_{3s}$ sequence and were consolidated in a hot platen press for 20 minutes at 370ºC and 10 bar pressure. The nominal consolidated thickness of each ply was 0.18 mm and that of the consolidated laminates was 2.16 mm. Coupons of sizes 120 mm x 40 mm and 180 mm x 100 mm were cut from the laminate for the welding trials using a water-cooled circular diamond saw. The coupons were cut with their longitudinal direction parallel to the 0^o direction of the laminates (see Figure 2). A 0.34 mm-thick discontinuous low-melt PAEK film was used as an energy director between the two adherends. The energy director was placed over the entire overlap area to make the sequential welding process easier to automate. The combination of the upper adherend, energy director and lower adherend is hereafter referred to as the welding stack. All coupons were cleaned with isopropanol to remove grease and other contaminants before welding.

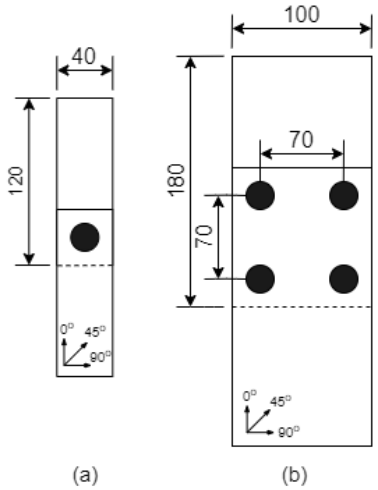

Figure 2. Schematic representation of single lap shear specimens in (a) single-spot and (b) multi-spot configurations (dimensions in mm)

Faculty of Aerospace Engineering, Delft University of Technology, Kluyverweg 1 2629HS Delft,The Netherlands

Static welding procedure

To produce the spot welds using the static process, a Rinco Ultrasonics Dynamic 3000 table-top welding machine (see Figure 3a) operating at a frequency of 20 kHz was used. The welding machine consists of an ultrasonic train which comprises a convertor, a booster and a sonotrode, being acted upon by a pneumatic press. The ultrasonic train in the static welding machine is encapsulated and clamped inside a closed box carriage on rails, hence not allowing any deflections of the ultrasonic train during the welding process except for vertical movement along a linear track, due to pressure applied by the press. A cylindrical 20 mm-diameter sonotrode was used to produce the circular welded spots. Based on pre-determined parameters from a preliminary study, each spot was welded with 800 N welding force and 65.8 μm peak-to-peak vibration amplitude. A vibration-time based welding control method was used. The ultrasonic vibrations begin when a force value called the trigger force is applied by the sonotrode. The optimal weld time for each weld spot was defined depending on the size of the adherends and on the location of the weld within the overlap. This was done by combining trial-and-error method with the analysis of time-resolved power and vertical displacement feedback obtained from the welder as well as of the fracture surfaces of the resultant welds. The consolidation time and force after the vibration phase were kept constant at 4s and 800N, respectively. The specimens were fixed in position during welding with the use of a bar-clamp based jig. The methodology for determining optimum weld parameters is not discussed in-depth in this paper, as the focus is on comparison between the static and robotic welding process, based on similar welding parameters.

Single-spot welds were performed in the configuration shown in Figure 2(a), with a 40 mm x 40 mm overlap area. Multi-spot welds were performed in a 4-spot square configuration, as shown in Figure 2(b) with a 100 mm x 100 mm overlap area. The 4-spot square configuration was studied in particular due to the intended application of the sequential ultrasonic welding process for welding structural clips to longitudinal stringers and fuselage skin (see Figure 1), in the multi-functional fuselage demonstrator. Welds were placed in a square pattern with each weld spaced 70 mm centre-to-centre from each other, in order to simulate the minimum spacing between weld spots in the clip-skin-stringer joint (see Figure 1) and to study the influence of adjacent welded spots on the sequential welding process and on the quality of welds. While welding with the static table-top machine, multi-spot welds were produced by manually moving the adherends on the jig relative to the fixed position of the sonotrode, to produce the welds sequentially.

Robotic welding hardware and procedure

The robotic welding hardware comprises an end-effector (EEF) mounted on a KUKA KR210 R2700 Extra industrial robot arm (see Figure 3b). The EEF includes an ultrasonic train fixed to an open box carriage mounted on linear guide rails as well as a pneumatic press capable of introducing a force up to 2 kN during the welding process. The ultrasonic train is lowered when pneumatic pressure is applied by the press. Unlike, the static welding machine, the ultrasonic train of the EEF is clamped to an open box carriage with a clamping block instead of it being completely encapsulated. The expected consequence of that is that the ultrasonic train would exhibit a higher

Faculty of Aerospace Engineering, Delft University of Technology, Kluyverweg 1 2629HS Delft,The Netherlands

Figure 3. Overview of welding hardware: (a) Static table-top machine (1. pneumatic press, 2. closed box carriage on rails and 3. ultrasonic train with sonotrode visible) and (b) EEF setup outlined in white on the KUKA KR210 R2700 Extra robot (4. pneumatic press, 5. open box carriage on rails and 6. ultrasonic train)

compliance under the application of high forces during the welding process as compared to that of the static welding machine. A 20 kHz Rinco Ultrasonics generator with a maximum power output of 3kW is used to generate the ultrasonic signal. All measured values from the displacement and pressure sensor in the end-effector are recorded at a sampling rate of 1kHz. The power dissipated during the welding process is recorded at a sampling rate of 100 Hz by the ultrasonic generator.

The welding process and parameters used while welding with the EEF were approximately the same as the static welding process. The main difference in the welding procedure as compared to the static welding procedure was that for the sequentially welded joints, the robot arm and hence the attached EEF moved relative to the fixed weld jig, in order to sequentially position the sonotrode above the intended weld spot(s). The general pose of the robot during the welding trials conducted in this study can be seen in Figure 3(b), with the EEF positioned perpendicularly above the surface of the welding jig and welding table. The Tool Centre Point (TCP) was defined at the lower tip of the sonotrode and the robot was programmed to ensure that the sonotrode remained perpendicular to the welding stack when the arm moved to reach each programmed position.

Robot position accuracy measurement

For the KUKA robot used in this study, a pose repeatability of 0.06 mm can be achieved. Due to the limited stiffness of robotic arms, as compared to a table-top static machine, it is necessary to characterize the deflection taking place during the welding process, in order to evaluate the difference in both processes. Hence, during the robotic welding process, the deflections of the robotic arm were captured. For recording the deflections, the robot is equipped with a Robot Sensor Interface (RSI) software package that enables capturing the position of the robot wrist at a sampling rate of 250 Hz.

Faculty of Aerospace Engineering, Delft University of Technology, Kluyverweg 1 2629HS Delft,The Netherlands

Testing and Microscopy
Single lap shear tests were performed to assess the mechanical performance of the welded joints. A Zwick/Roell 250 kN universal testing machine with hydraulic grips, operated at 1.3 mm/min cross-head speed and under displacement control was used for the single lap shear tests. Five samples were tested per single-spot and multi-spot welding configuration for each of the processes. A Keyence VR-5000 Wide Area 3D measuring system was used to measure the welded surface area and analyse the failure mechanism of the welds after single-lap shear testing.

RESULTS AND DISCUSSION

In this section, the results obtained from the position measurement of the robot arm and the power-displacement feedback obtained from the welding EEF during the welding process; as well as the weld quality results in terms of single lap shear strength and welded area are presented and discussed. The weld quality assessment of the welds produced through the robotic process is done by comparing it to the quality of welds produced through the static table-top welding process.

Robot position accuracy
The position of the robot arm at the beginning of the vibration phase and deflections during the vibration phase are of importance, as they influence the contact angle between the sonotrode and the upper adherend and ultimately the transmission of mechanical vibrations into the joint. The side schematic view of the robotic welding hardware shown in Figure 4 indicates the global frame of reference used. Figure 5 and the close-up in Figure 6, show representative position data of the robot arm, measured at the wrist of the robot during the spot welding experiments. The deflections are computed relative to the nominal position of the robot wrist for the welding process. The sequence of deflections of the system during the different phases of the welding process are explained below:

1. During the force build-up phase, and due to the force applied on the welding stack by the sonotrode, a reaction moment is generated at the robot wrist, causing a deflection of the wrist in the X and Z directions. The dynamic control of the robot arm aims at correcting the X-Z deflection of the robot wrist by moving the wrist in the direction opposite to the initial deflection, as shown by the decrease in X and Z displacements towards the end of the force build-up phase in Figure 5.

2. The vibration phase begins when a stable force value of 800N which is defined as the trigger force, is reached. Due to the very short duration of the force build-up phase, the robot wrist has not returned to its programmed X and Z position when the vibrations start. As the energy director begins melting, the sonotrode moves downwards in the vertical direction as the thickness of the welding stack decreases. This allows for the robot wrist to correct its position further by aiming to approach the nominal Z position, as can be clearly seen in Figure 6.

Faculty of Aerospace Engineering, Delft University of Technology, Kluyverweg 1 2629HS Delft,The Netherlands

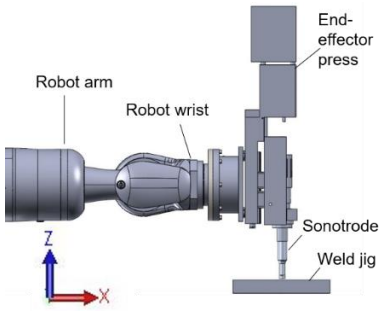

Figure 4. Schematic side view of the robot welding equipment (global frame of reference indicated)

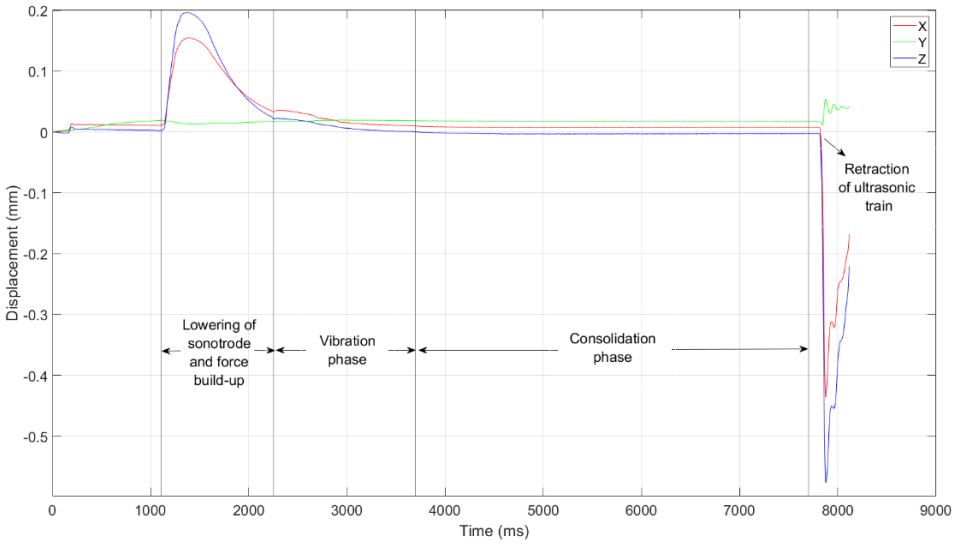

Figure 5. Representative deflection of robot arm (measured at the wrist) during different phases of the spot welding process

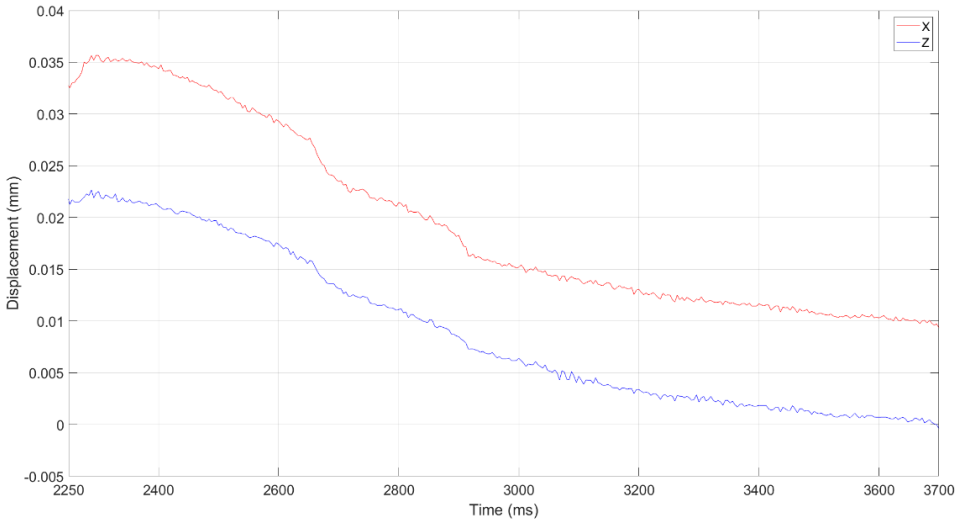

Figure 6. Representative X-Z Displacement of robot arm (measured at the wrist) during the vibration phase of spot welds (close-up of vibration phase from Figure 5)

3. During the consolidation phase, the vibrations stop and a uniform force is applied by the sonotrode. Hence, during this phase the robot moves back to its

Faculty of Aerospace Engineering, Delft University of Technology, Kluyverweg 1 2629HS Delft,The Netherlands

programmed positon in the Z axis. A deflection of approximately 0.01 mm remains in the X-direction, which is deemed to be insignificant.

4. The ultrasonic train is retracted after the consolidation phase and a large displacement is captured in the X and Z direction as can be seen in Figure 5. However, this motion of the robot has no consequence on the welding process.

According to Figure 5 and 6, the displacements of the robot wrist along the X-direction and the Z-direction at the end of the vibration phase are approximately 0.01 mm and 0.00 mm, respectively. However, as observed on the welded coupons, the circular welded spot on the adherends is actually displaced 1 mm from the intended location, along the X-direction. We believe that this displacement is caused by bending taking place within the EEF, most likely at the joint between the carriage and the ultrasonic train, as the welding force is applied. This bending of the ultrasonic train results in the sonotrode sliding on the surface of the adherend and causing a certain deviation from the intended sonotrode position along the X-direction. During the force build-up face, bending is however restrained beyond a certain point due to friction at the interface between the sonotrode and the upper adherend. During the vibration phase, it is suspected that due to a reduction in the friction between the sonotrode and upper adherend the ultrasonic train is allowed to bend further and, consequently, the sonotrode further deflects along the X direction at the beginning of the vibration phase and then stabilizes ending up in the measured 1 mm displacement. This most likely also causes a vertical movement of the ultrasonic train along with the carriage, as the pneumatic press tries to stabilize the applied pressure value corresponding to 800 N force. The deflections which were visually observed in the EEF during the welding process in the form of bending, are independent of the robot system. However, the displacement data for the robot wrist suggests that minor deflections do occur in the robot arm during the welding process which potentially cause a minor misalignment of the EEF and consequently a suboptimal contact angle between the sonotrode and the welding stack. This deflection, although very small is expected to affect weld quality and spot positioning accuracy. A schematic representation of all the forces exerted during the welding process and the resulting deflections can be visualized in Figure 7.

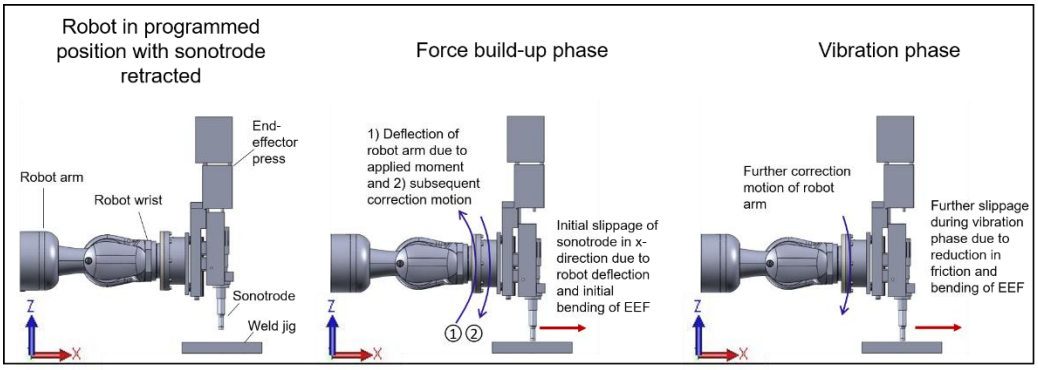

Figure 7. Overview of robot and EEF deflection during the spot welding process based on global frame of reference (side view)

Faculty of Aerospace Engineering, Delft University of Technology, Kluyverweg 1 2629HS Delft,The Netherlands

Power-displacement curves

The power and displacement data measured by the ultrasonic generator and the displacement sensor integrated in the EEF, respectively, are important to be analysed as they give information about the physical phenomena of melting and squeeze out and allow for a comparison of both welding processes, regardless of the external deflections of the system as discussed in the previous section. The sliding motion of the sonotrode that was observed in the beginning of the vibration phase of the robotic welding process is suspected to cause some energy dissipation, as the contact between the sonotrode and the welding stack is believed to be suboptimal.

In Figure 8, a comparison between the vertical displacement data of the ultrasonic train obtained from the internal sensor of the static welding machine and the EEF is presented. It can be seen that in the case of welds produced by the static process, from the beginning of the welding process till approximately 35 ms, a rapid increase in displacement is observed till a displacement of approximately 0.08mm is reached when the discontinuous energy director is flattened. However, in the case of the robotic welds, since the sonotrode slides due to the ultrasonic train bending, it is believed that the ultrasonic train along with the carriage moves vertically along the axis of the EEF, as a result of the pneumatic press trying to stabilize the applied pressure and hence a relatively large Z-displacement can be observed. The rapid increase in displacement of the sonotrode ends at a later stage during the vibrations, after approximately 75 ms and at 0.45 mm displacement. Since the ED thickness is 0.34 mm, this displacement value is clearly not due to the ED being flattened but rather due to the movement of the EEF. Following this, as the position of the sonotrode stabilizes while still vibrating, the trends of the displacement curves are similar, indicating that the welding process progresses similar to that of the static machine. Since, the process is time-controlled with similar vibration time used for both the static and robotic welds, the initial dissipation of energy due to movement of the sonotrode and the resulting suboptimal contact angle between the sonotrode and the welding stack, is suspected to result in the lower welded area in the robotic welds

The power consumption data obtained from the ultrasonic generators of the static and robotic welding process (see Figure 9) indicate that both processes exhibit broadly similar power consumption trends, with a peak power consumption in the range of 2000 W and 2500 W. The total energy consumed during the welding process for each spot was in the range of 2100 J and 2500 J. Slightly lower power peaks for the robotic process indicate that due to the initial movement of the sonotrode during the vibration phase of the robotic process as well as the reduced overall stiffness of the system, the transmission of mechanical vibrations into the welding stack is suboptimal as the ultrasonic train is more complaint and hence results in lower power consumption during the welding process. However, the power consumption data from the ultrasonic generator also indicates that both processes are quite comparable and some minor differences in the evolution of power consumption during the vibration phase can be attributed to the movement of the robot wrist as well as the bending within the EEF.

Faculty of Aerospace Engineering, Delft University of Technology, Kluyverweg 1 2629HS Delft,The Netherlands

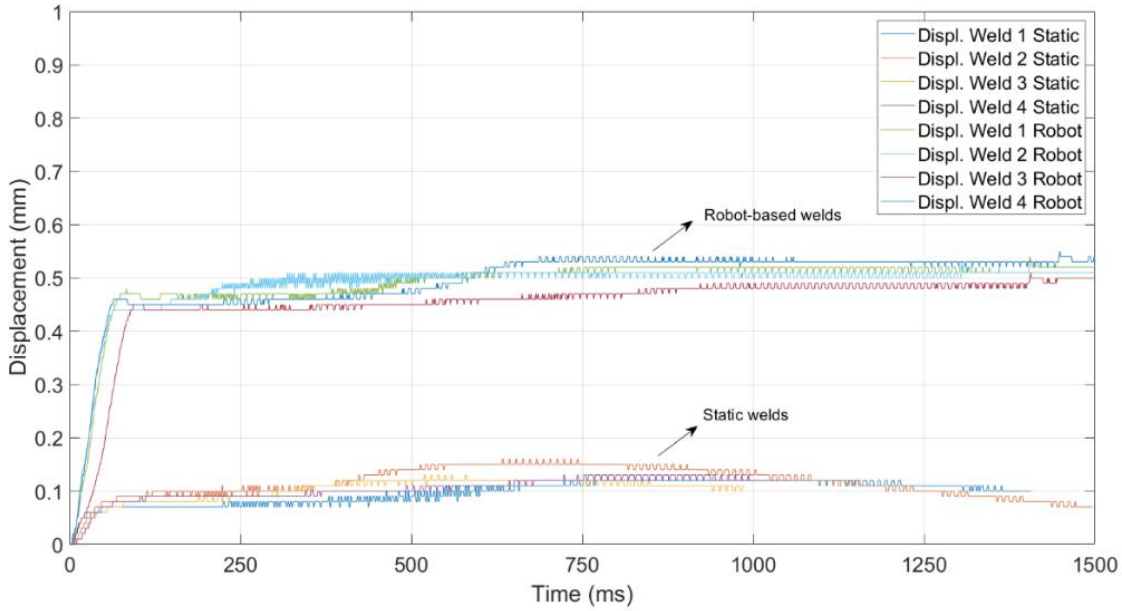

Figure 8. Representative sonotrode displacement data measured for static and robotic multi-spot welds (measured in the negative Z direction based on global frame of reference)

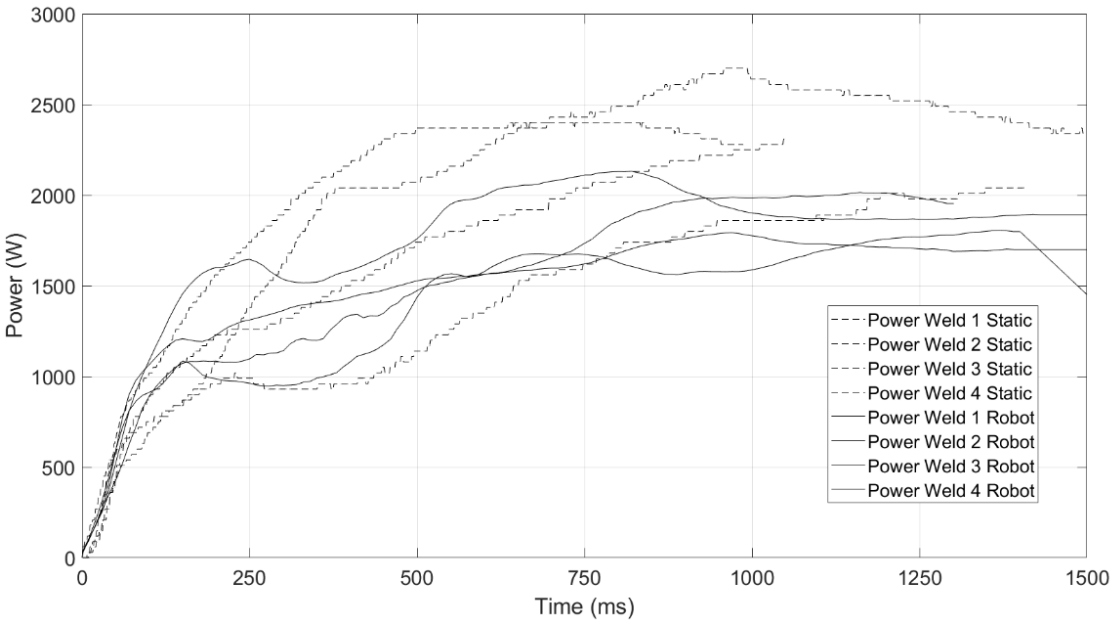

Figure 9. Representative power consumption data measured for static and robotic multi-spot welds

Single lap shear tests and fractography

In this sub-section, welds produced by the static and robotic welding process are described and compared. The fracture surface of representative static welds in single-spot and multi-spot configuration after single lap shear testing can be seen in Figure 10. Similar weld shape and fracture surfaces were obtained from welds produced through both static and robotic processes. Due to the fibre orientation at the interface ply and the resulting increased heat transfer along the 0^o fibre orientation, each resulting welded spot has an elliptical shape. During lap-shear testing, failure was observed to occur in the first-ply in all samples, indicating high weld quality. In Table

Faculty of Aerospace Engineering, Delft University of Technology, Kluyverweg 1 2629HS Delft,The Netherlands

I, the total Welded Area (WA), Ultimate Failure Load (UFL) and average UFL/number of spots for the single- and multi-spot welds obtained with both the static and robotic process is presented. It can be observed that due to the joint configuration of the multi-spot welds, wherein the load distribution on the four spots is not optimal during tensile shear testing, the ultimate failure load per spot of the joint is lower than that in the case of the single-spot joint configuration. Furthermore, slightly lower weld area and consequently lower ultimate failure strength were observed for the welds obtained using the robotic process, however the difference is not large. These results indicate that the welding process is quite robust despite the deflections observed in both the robot wrist and the end-effector due to the high process forces. Although, a large X deflection of the sonotrode of 1 mm was visually observed by the final position of the welded spot on the welding stack and a large Z displacement of the sonotrode was observed from the displacement data of the ultrasonic train (see Figure 8), the weld quality obtained from both processes is quite comparable. The slightly lower welded area obtained for the welds produced with the robotic process, can be attributed to the lower power consumption originating from the suboptimal contact angle between the sonotrode and the weld stack. Since, the process is time-controlled with similar vibration time used for both the static and robotic welds, the initial dissipation of energy due to movement of the sonotrode and the resulting suboptimal contact between the sonotrode and the welding stack, is suspected to result in the lower welded area in the robotic welds. Hence, the deflections of the robotic system, including the robot arm and the EEF, result in a lower albeit comparable weld quality.

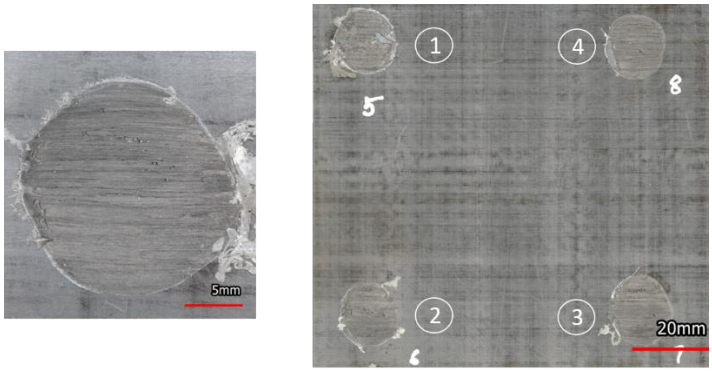

(a) (b)

Figure 10. Representative weld fracture surfaces obtained after single lap shear testing in (a) single-spot configuration and (b) multi-spot configuration with weld sequence denoted as 1,2,3 and 4 respectively

TABLE I. WELDED AREA (WA) AND ULTIMATE FAILURE LOAD (UFL) (n=5)

Weld configuration	**Total WA (mm^2)**	**UFL (N)**	**Average UFL/spot (N)**
Static single-spot	308.3 ± 6.8	11623 ± 414	11623
Robotic single-spot	290.4 ± 12.2	11325 ± 440	11325
Static multi-spot	949 ± 48.4	35002 ± 1976	8750.5
Robotic multi-spot	933.4 ± 52.2	33979 ± 1721	8494.7

Faculty of Aerospace Engineering, Delft University of Technology, Kluyverweg 1 2629HS Delft,The Netherlands

CONCLUSION

In this study, the welding behaviour and attributes of sequentially welded spots on thermoplastic composite laminates, produced by a robotic multi-spot sequential ultrasonic welding process, were experimentally determined and compared to those produced by a static table-top welding machine. An ultrasonic welding end-effector and welding process were developed and based on weld parameters comparable to the static welding process, single and multi-spot welds were produced on thermoplastic composite coupons. The coupons were manufactured from uni-direction pre-impregnated CF LMPAEK tapes.

The main conclusion drawn from this work is that despite the fact that significant deflections were observed during the robotic welding process, due to a combination of limited stiffness of the robot arm as well as the internal bending of the EEF about its frame, the resulting weld quality was found to be comparable between the two processes for a similar set of welding parameters. Based on this study, some recommendations to improve the developed end-effector and the welding process for industrial application were devised and can be summarized as follows:

- For the current robotic process, since a significant sonotrode deflection takes place at the beginning of the welding process resulting in dissipation of weld energy, an optimized set of welding parameters need to be determined for the robotic process, in order to improve weld quality.

- The clamping of the ultrasonic train to the carriage and the frame of the EEF needs to be reinforced, in order to avoid bending of the ultrasonic train under high force application. This would reduce the sonotrode deflection and ensure perpendicularity of the sonotrode to the welding stack during the welding process. Furthermore, this is expected to improve the positioning accuracy of the welded spot as well as the measured displacement data of the ultrasonic train.

- Use of a stiffer robotic platform would reduce the initial deflection of the robot arm, hence increasing accuracy in positioning and of the sensor feedback

ACKNOWLEDGEMENT

This project has received funding from the Clean Sky 2 Joint Undertaking (JU) under grant agreement No 945583. The JU receives support from the European Union's Horizon 2020 research and innovation programme and the Clean Sky 2 JU members other than the Union.

Furthermore, the authors would like to acknowledge the contribution of Berthil Grashof, André Florindo and Rik Tonnaer who helped immensely in setting up the PLC for the robotic end-effector.

Faculty of Aerospace Engineering, Delft University of Technology, Kluyverweg 1 2629HS Delft,The Netherlands

DISCLAIMER

The results, opinions, conclusions, etc. presented in this work are those of the author(s) only and do no do not necessarily represent the position of the JU; the JU is not responsible for any use made of the information contained herein.

REFERENCES

1. I.F. Villegas, L. Moser, A. Yousefpour, P. Mitschang, and H.E.N. Bersee. Process and performance evaluation of ultrasonic, induction and resistance welding of advanced thermoplastic composites. Journal of Thermoplastic Composite Materials, 26(8):1007– 1024, 2013.
2. D. Grewell, A. Benatar, and Joon B Park. Plastics and composites welding handbook, volume 10. 2003
3. Ageorges C, Ye L and Hou M. Advances in fusion bond-ing techniques for joining thermoplastic matrix compo- sites: a review. Composites Part A 2001; 32: 839–857.
4. I.F. Villegas. Ultrasonic Welding of Thermoplastic Composites. Front. Mater. 6:291, 2019.
5. H. Potente. Ultrasonic welding - principles & theory. Materials & Design, 5(5):228 – 234, 1984.
6. Zhou et al., 2019, “On sequential ultrasonic spot welding as an alternative to mechanical fastening in thermoplastic composite assemblies: A study on single-column multi-row single-lap shear joints”, Composites Part A: Applied Science and Manufacturing, Pg. 1-11.
7. T. Zhao, G. Palardy, I.F. Villegas, C. Rans, M. Martinez, and R. Benedictus. Mechanical behaviour of thermoplastic composites spot-welded and mechanically fastened joints: A preliminary comparison. Composites Part B: Engineering, 112:224–234, 2017.
8. S.L. Veldman et al. “Development of a multifunctional fuselage demonstrator”. Proceedings of Aerospace Europe Conference, Bordeaux, 2020.

Faculty of Aerospace Engineering, Delft University of Technology, Kluyverweg 1 2629HS Delft,The Netherlands